Supporting Information

Facile Incorporation of Au Nanoparticles into an Unusual Twofold Entangled Zn(II)-MOF with Nanocages for Highly Efficient CO_2 Fixation under Mild Conditions

Yun-Long Wu,[†,‡,⊥] Guo-Ping Yang,*[,†,∥,⊥] Shan Cheng,[†] Jinjie Qian,[§] Daidi Fan,[∥] and Yao-Yu Wang*[,†]

[†]Key Laboratory of Synthetic and Natural Functional Molecule Chemistry of Ministry of Education, Shaanxi Key Laboratory of Physico-Inorganic Chemistry, College of Chemistry & Materials Science, and [∥]School of Chemical Engineering, Northwest University, Xi'an 710127, P.R. China;

[‡]School of Materials Science & Engineering, Xi'an Polytechnic University, Xi'an, 710048, P. R. China;

[§]College of Chemistry & Materials Engineering, Wenzhou University, Wenzhou, 325035, P. R. China.

Corresponding Authors: *E-mail: ygp@nwu.edu.cn; wyaoyu@nwu.edu.cn.

Contents

I Tables

Table S1. Crystal data and structure refinements for MOF **1**.

Complex	**1**
Empirical formula	$Zn_{14}C_{126}H_{60}N_6O_{55}$
Formula mass	3453.26
Crystal system	Trigonal
Space group	R-3m
a [Å]	34.4562(7)
b [Å]	34.4562 (7)
c [Å]	38.7960(5)
α [°]	90
β [°]	90
γ [°]	120
V [Å^3]	39888.9(17)
Z	9
$D_{calcd.}$[g·cm^{-3}]	1.294
μ [mm^{-1}]	1.928
F [000]	15460
θ [°]	0.861-24.712
Reflections collected	65184 / 7963
Goodness-of-fit on F^2	1.301
Final $R^{[a]}$ indices [I>2σ(I)]	R1 = 0.0986, wR2 = 0.3135

[a] $R_1=\sum||F_o|-|F_c||/\sum|F_o|$, $wR_2=[\sum w(F_o^2- F_c^2)^2/ \sum w(F_o^2)^2]^{1/2}$

Table S2. Selected bonds lengths [Å] and angles [°] of **1**.

MOF 1			
Zn(4)-Zn(1)#1	3.307(3)	O(10)-Zn(3)-O(6)	112.6(3)
Zn(4)-Zn(3)#2	3.2630(18)	O(10)-Zn(3)-O(1)#1	104.7(4)
Zn(4)-Zn(3)	3.2630(18)	O(10)-Zn(3)-O(5)	105.9(4)
Zn(4)-O(6)	1.985(8)	O(3)-Zn(2)-Zn(5)	78.0(2)
Zn(4)-O(7)#2	1.941(6)	O(3)#7-Zn(2)-Zn(5)	78.0(2)
Zn(4)-O(7)	1.941(6)	O(3)-Zn(2)-O(3)#7	88.5(4)
Zn(4)-O(8)#3	1.982(11)	O(4)#7-Zn(2)-Zn(5)	79.4(2)
Zn(1)-Zn(4)#3	3.307(3)	O(4)-Zn(2)-Zn(5)	79.4(2)
Zn(1)-Zn(3)#4	3.178(2)	O(4)#7-Zn(2)-O(3)	157.4(3)
Zn(1)-Zn(3)#3	3.178(2)	O(4)-Zn(2)-O(3)	86.3(3)
Zn(1)-O(6)#3	1.995(8)	O(4)-Zn(2)-O(3)#7	157.4(3)
Zn(1)-O(2)#5	2.004(9)	O(4)#7-Zn(2)-O(3)#7	86.4(3)
Zn(1)-O(2)	2.004(9)	O(4)-Zn(2)-O(4)#7	90.0(3)
Zn(1)-O(9)#6	2.035(14)	O(14)-Zn(2)-Zn(5)	179.9(5)
Zn(3)-Zn(1)#1	3.178(2)	O(14)-Zn(2)-O(3)#7	102.1(3)

Zn(3)-Zn(3)#2	3.145(2)	O(14)-Zn(2)-O(3)	102.1(3)
Zn(3)-O(6)	1.959(5)	O(14)-Zn(2)-O(4)	100.5(3)
Zn(3)-O(1)#1	1.918(7)	O(14)-Zn(2)-O(4)#7	100.5(3)
Zn(3)-O(5)	1.919(7)	O(12)#7-Zn(5)-Zn(2)	79.0(2)
Zn(3)-O(10)	1.907(8)	O(12)-Zn(5)-Zn(2)	79.0(2)
Zn(2)-Zn(5)	3.019(2)	O(12)-Zn(5)-O(12)#7	89.7(4)
Zn(2)-O(3)#7	2.045(7)	O(12)#7-Zn(5)-O(11)#7	86.1(3)
Zn(2)-O(3)	2.045(7)	O(12)-Zn(5)-O(11)#7	157.0(3)
Zn(2)-O(4)#7	2.035(6)	O(12)-Zn(5)-O(11)	86.1(3)
Zn(2)-O(4)	2.035(6)	O(12)#7-Zn(5)-O(11)	157.0(3)
Zn(2)-O(14)	1.954(11)	O(13)-Zn(5)-Zn(2)	179.5(3)
Zn(5)-O(12)#7	2.027(7)	O(13)-Zn(5)-O(12)	100.6(3)
Zn(5)-O(12)	2.027(7)	O(13)-Zn(5)-O(12)#7	100.6(3)
Zn(5)-O(13)	1.927(10)	O(13)-Zn(5)-O(11)#7	102.3(3)
Zn(5)-O(11)	2.039(6)	O(13)-Zn(5)-O(11)	102.3(3)
Zn(5)-O(11)#7	2.039(6)	O(11)#7-Zn(5)-Zn(2)	78.0(2)
Zn(6)-C(34)#10	2.42(2)	O(11)-Zn(5)-Zn(2)	78.0(2)
Zn(6)-Zn(6)#10	2.067(8)	O(11)-Zn(5)-O(11)#7	89.1(5)
Zn(6)-Zn(6)#9	2.066(8)	C(34)#10-Zn(6)-Zn(7)	164.4(6)
Zn(6)-Zn(7)#9	2.266(6)	O(15)-Zn(6)-C(34)#10	90.5(7)
Zn(6)-Zn(7)#10	2.266(6)	O(15)-Zn(6)-Zn(6)#10	126.6(6)
Zn(6)-Zn(7)	3.029(7)	O(15)-Zn(6)-Zn(6)#9	84.5(6)
Zn(6)-C(40)#10	1.13(2)	O(15)-Zn(6)-Zn(7)#9	79.1(5)
Zn(6)-O(18)	2.09(2)	O(15)-Zn(6)-Zn(7)	78.3(6)
Zn(7)-C(29)#9	1.155(19)	O(15)-Zn(6)-Zn(7)#10	38.2(6)
Zn(7)-Zn(6)#9	2.266(6)	O(15)-Zn(6)-O(18)	87.1(9)
Zn(7)-Zn(6)#10	2.266(6)	Zn(6)#9-Zn(6)-C(34)#10	142.1(3)
Zn(7)-Zn(7)#9	1.956(8)	Zn(6)#10-Zn(6)-C(34)#10	142.1(3)
Zn(7)-Zn(7)#10	1.956(8)	Zn(6)#9-Zn(6)-Zn(6)#10	60.000(2)
Zn(7)-O(19)	2.07(2)	Zn(6)#9-Zn(6)-Zn(7)#9	88.60(14)
Zn(3)-Zn(4)-Zn(1)#1	57.86(5)	Zn(6)#10-Zn(6)-Zn(7)	48.40(8)
Zn(3)#2-Zn(4)-Zn(1)#1	57.86(5)	Zn(6)#9-Zn(6)-Zn(7)	48.41(8)
Zn(3)#2-Zn(4)-Zn(3)	57.63(5)	Zn(6)#9-Zn(6)-Zn(7)#10	62.87(12)
O(6)-Zn(4)-Zn(1)#1	33.9(2)	Zn(6)#10-Zn(6)-Zn(7)#10	88.60(14)
O(6)-Zn(4)-Zn(3)#2	33.92(11)	Zn(6)#10-Zn(6)-Zn(7)#9	62.88(12)
O(6)-Zn(4)-Zn(3)	33.92(11)	Zn(6)#10-Zn(6)-O(18)	84.4(6)
O(7)#2-Zn(4)-Zn(1)#1	123.5(2)	Zn(6)#9-Zn(6)-O(18)	35.0(6)
O(7)-Zn(4)-Zn(1)#1	123.5(2)	Zn(7)#10-Zn(6)-C(34)#10	127.3(5)
O(7)#2-Zn(4)-Zn(3)#2	76.5(2)	Zn(7)#9-Zn(6)-C(34)#10	127.3(5)
O(7)-Zn(4)-Zn(3)#2	123.2(2)	Zn(7)#10-Zn(6)-Zn(7)	40.19(16)
O(7)-Zn(4)-Zn(3)	76.5(2)	Zn(7)#9-Zn(6)-Zn(7)	40.20(16)
O(7)#2-Zn(4)-Zn(3)	123.2(2)	Zn(7)#9-Zn(6)-Zn(7)#10	51.1(2)
O(7)-Zn(4)-O(6)	110.4(2)	C(40)#10-Zn(6)-C(34)#10	5.2(18)
O(7)#2-Zn(4)-O(6)	110.4(2)	C(40)#10-Zn(6)-O(15)	86.8(14)

O(7)#2-Zn(4)-O(7)	108.3(4)	C(40)#10-Zn(6)-Zn(6)#9	144.9(8)
O(7)-Zn(4)-O(8)#3	107.1(3)	C(40)#10-Zn(6)-Zn(6)#10	144.9(9)
O(7)#2-Zn(4)-O(8)#3	107.1(3)	C(40)#10-Zn(6)-Zn(7)	159.2(17)
O(8)#3-Zn(4)-Zn(1)#1	79.4(5)	C(40)#10-Zn(6)-Zn(7)#10	122.9(15)
O(8)#3-Zn(4)-Zn(3)#2	125.9(4)	C(40)#10-Zn(6)-Zn(7)#9	122.9(15)
O(8)#3-Zn(4)-Zn(3)	125.9(4)	C(40)#10-Zn(6)-O(18)	110.7(13)
O(8)#3-Zn(4)-O(6)	113.3(5)	O(18)-Zn(6)-C(34)#10	107.4(7)
Zn(3)#3-Zn(1)-Zn(4)#3	60.38(5)	O(18)-Zn(6)-Zn(7)	83.2(6)
Zn(3)#4-Zn(1)-Zn(4)#3	60.38(5)	O(18)-Zn(6)-Zn(7)#9	123.2(6)
Zn(3)#3-Zn(1)-Zn(3)#4	59.32(6)	O(18)-Zn(6)-Zn(7)#10	85.7(7)
O(6)#3-Zn(1)-Zn(4)#3	33.7(2)	C(29)#9-Zn(7)-O(16)	114.2(10)
O(6)#3-Zn(1)-Zn(3)#3	36.11(13)	C(29)#9-Zn(7)-O(17)	23.9(17)
O(6)#3-Zn(1)-Zn(3)#4	36.11(13)	C(29)#9-Zn(7)-Zn(6)#9	117.8(10)
O(6)#3-Zn(1)-O(2)	98.2(3)	C(29)#9-Zn(7)-Zn(6)	156.3(12)
O(6)#3-Zn(1)-O(2)#5	98.2(3)	C(29)#9-Zn(7)-Zn(6)#10	117.8(10)
O(6)#3-Zn(1)-O(9)#6	104.2(6)	C(29)#9-Zn(7)-Zn(7)#10	146.2(5)
O(2)#5-Zn(1)-Zn(4)#3	102.3(3)	C(29)#9-Zn(7)-Zn(7)#9	146.2(5)
O(2)-Zn(1)-Zn(4)#3	102.3(3)	C(29)#9-Zn(7)-O(19)	80.0(11)
O(2)-Zn(1)-Zn(3)#4	123.0(3)	O(16)-Zn(7)-Zn(6)#10	124.9(5)
O(2)#5-Zn(1)-Zn(3)#3	123.0(3)	O(16)-Zn(7)-Zn(6)#9	86.3(5)
O(2)#5-Zn(1)-Zn(3)#4	65.1(3)	O(16)-Zn(7)-Zn(6)	82.0(5)
O(2)-Zn(1)-Zn(3)#3	65.1(3)	O(17)-Zn(7)-O(16)	93.5(19)
O(2)-Zn(1)-O(2)#5	154.5(7)	O(17)-Zn(7)-Zn(6)#10	140.8(17)
O(2)#5-Zn(1)-O(9)#6	97.4(3)	O(17)-Zn(7)-Zn(6)	173(2)
O(2)-Zn(1)-O(9)#6	97.4(3)	O(17)-Zn(7)-Zn(6)#9	131.4(17)
O(9)#6-Zn(1)-Zn(4)#3	70.5(5)	O(17)-Zn(7)-O(19)	90.9(18)
O(9)#6-Zn(1)-Zn(3)#4	120.5(4)	Zn(6)#10-Zn(7)-Zn(6)	43.00(17)
O(9)#6-Zn(1)-Zn(3)#3	120.5(4)	Zn(6)#9-Zn(7)-Zn(6)	42.99(17)
Zn(1)#1-Zn(3)-Zn(4)	61.76(5)	Zn(6)#10-Zn(7)-Zn(6)#9	54.3(2)
Zn(3)#2-Zn(3)-Zn(4)	61.19(2)	Zn(7)#9-Zn(7)-O(16)	82.3(5)
Zn(3)#2-Zn(3)-Zn(1)#1	60.34(3)	Zn(7)#10-Zn(7)-O(16)	33.7(5)
O(6)-Zn(3)-Zn(4)	34.4(2)	Zn(7)#9-Zn(7)-O(17)	136.8(15)
O(6)-Zn(3)-Zn(1)#1	36.9(2)	Zn(7)#10-Zn(7)-O(17)	127.2(19)
O(6)-Zn(3)-Zn(3)#2	36.59(19)	Zn(7)#10-Zn(7)-Zn(6)#10	91.40(14)
O(1)#1-Zn(3)-Zn(4)	130.3(3)	Zn(7)#10-Zn(7)-Zn(6)#9	64.43(11)
O(1)#1-Zn(3)-Zn(1)#1	83.3(3)	Zn(7)#9-Zn(7)-Zn(6)	48.40(8)
O(1)#1-Zn(3)-Zn(3)#2	130.8(3)	Zn(7)#9-Zn(7)-Zn(6)#10	64.44(11)
O(1)#1-Zn(3)-O(6)	120.1(3)	Zn(7)#9-Zn(7)-Zn(6)#9	91.40(14)
O(1)#1-Zn(3)-O(5)	104.9(4)	Zn(7)#10-Zn(7)-Zn(6)	48.40(8)
O(5)-Zn(3)-Zn(4)	73.1(2)	Zn(7)#10-Zn(7)-Zn(7)#9	60.000(2)
O(5)-Zn(3)-Zn(1)#1	124.4(2)	Zn(7)#10-Zn(7)-O(19)	87.3(6)
O(5)-Zn(3)-Zn(3)#2	122.4(2)	Zn(7)#9-Zn(7)-O(19)	131.7(8)
O(5)-Zn(3)-O(6)	107.5(3)	O(19)-Zn(7)-O(16)	88.5(9)
O(10)-Zn(3)-Zn(4)	123.9(3)	O(19)-Zn(7)-Zn(6)#10	83.6(9)

O(10)-Zn(3)-Zn(1)#1	125.3(3)	O(19)-Zn(7)-Zn(6)	83.4(8)
O(10)-Zn(3)-Zn(3)#2	76.1(3)	O(19)-Zn(7)-Zn(6)#9	40.5(8)

Symmetry codes: #1: -y+2/3, x-y+1/3, z+1/3; #2: -y+1, -x+1, z; #3: -x+y+1/3, -x+2/3, z-1/3; #4: -x+y+1/3, y-1/3, z-1/3; #5: x, x-y, z; #6: -y+2/3, x-y+1/3, z-2/3; #7: -x+y, y, z; #8: -x+y+1/3, -x+2/3, z+2/3; #9: -y+1, x-y+1, z; #10: -x+y, -x+1, z.

Table S3. Cycloaddition of CO_2 under the same conditions containing different catalysts

Entry	Catalysts	Epoxides	Products	Yields
1	Au@**1**	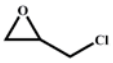		0
2	**1**/TBAB	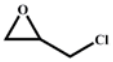		~10%
3	Au@**1**/TBAB	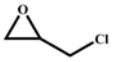		>99%

Reaction condition: 2-(chloromethyl)oxirane (20 mmol); Au@**1**/**1** (0.1 mmol); TBAB (2 mmol); gas: CO_2 containing balloon; reaction 80 °C / 8h)

II Figures

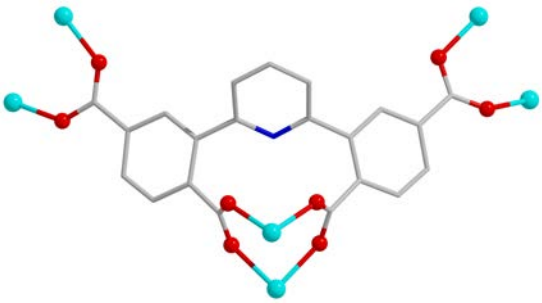

Figure S1. The coordination mode of L^{4-} in MOF **1**: the carboxylate groups adopt one bridging bidentate $\eta^2\mu_2\chi^2$ coordination mode.

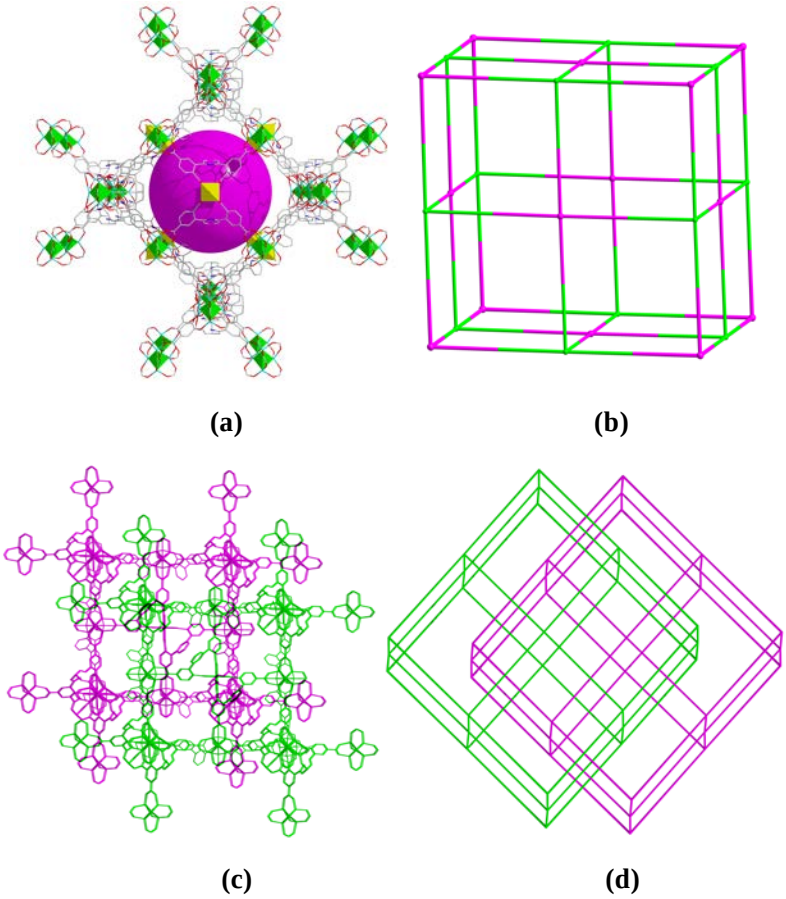

Figure S2. (a) one fold 3D porous network of **1**; (b) One fold 3D topology network of **1**; (c) 3D-two overlapping cage of **1**; (d) The topology network of **1**.

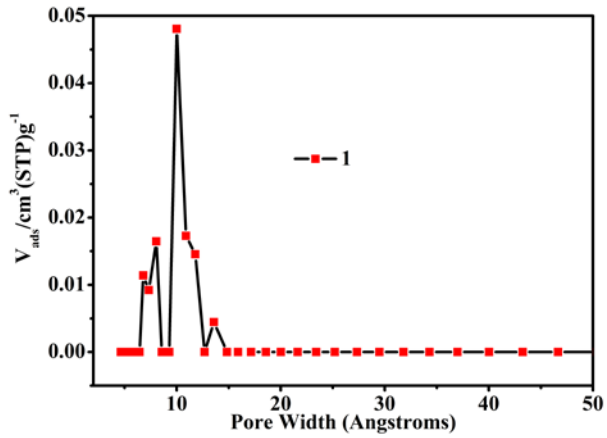

(a)

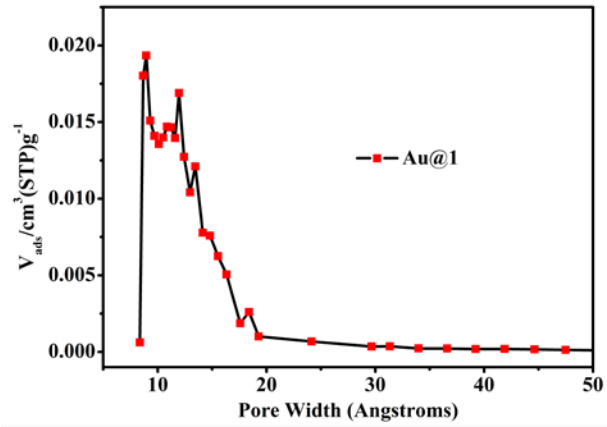

(b)

Figure S3. The pore size distribution in **1** (a) and Au@**1** (b).

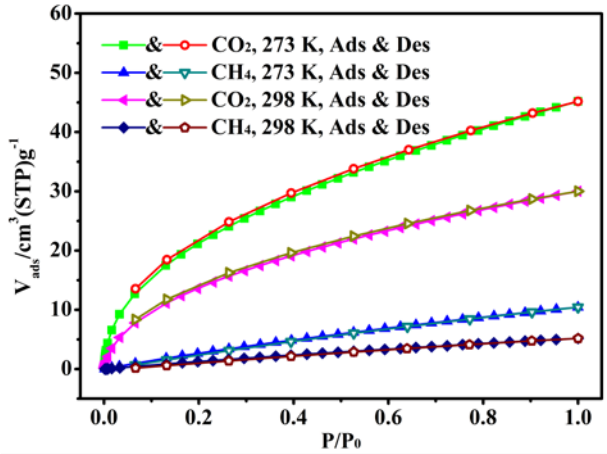

(a)

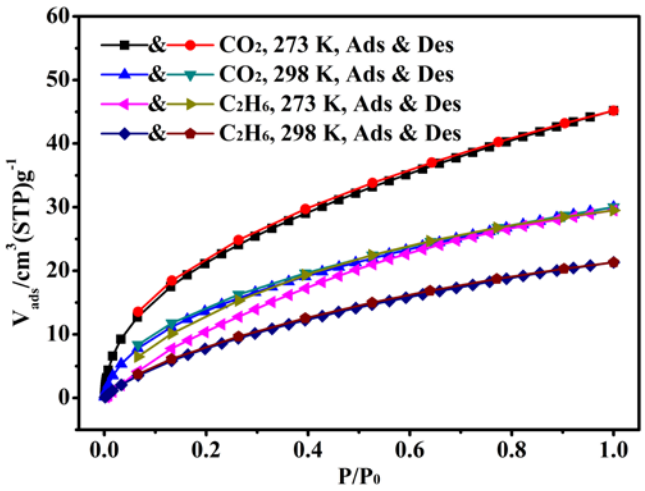

(b)

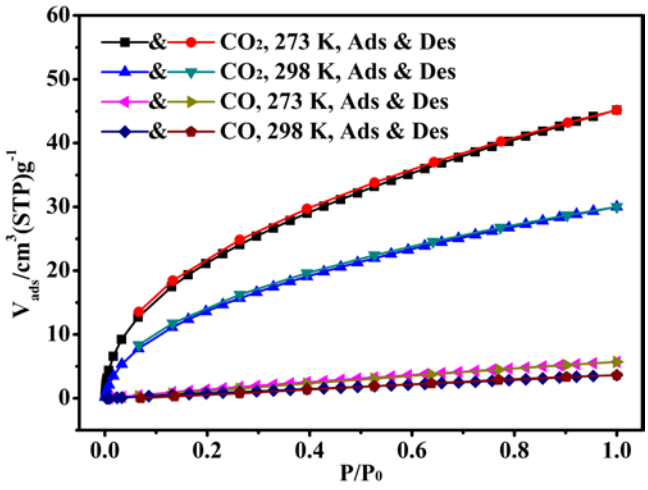

(c)

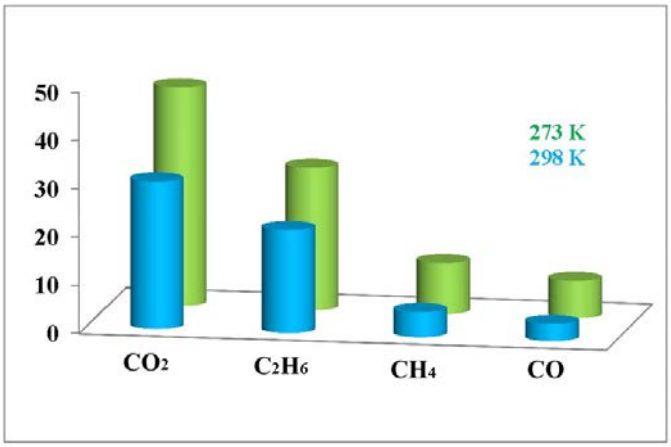

(d)

Figure S4. (a), (b), (c) $CO_2/CH_4/C_2H_6/CO$ sorption isotherms of **1** at 273 and 298 K; (d) The maximum adsorbed amounts comparison of **1** at 273 and 298 K.

IAST adsorption selectivity calculation:

The experimental isotherm data for pure CO_2 and CH_4 (measured at 273 and 298 K) were fitted using a Langmuir-Freundlich (L-F) model:

$$q = \frac{a * b * p^c}{1 + b * p^c}$$

Where q and p are adsorbed amounts and pressures of component i, respectively. The adsorption selectivities for binary mixtures of CO_2/CH_4 at 273 and 298 K, defined by

$$S_{ads} = (q_1 / q_2) / (p_1 / p_2)$$

Where qi is the amount of i adsorbed and pi is the partial pressure of i in the mixture.

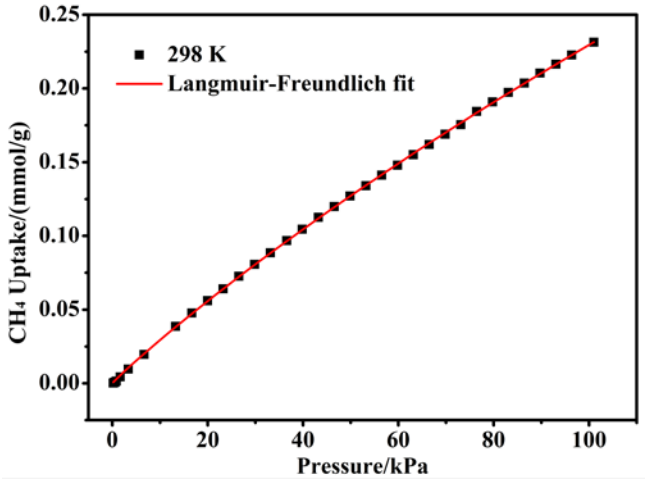

(a)

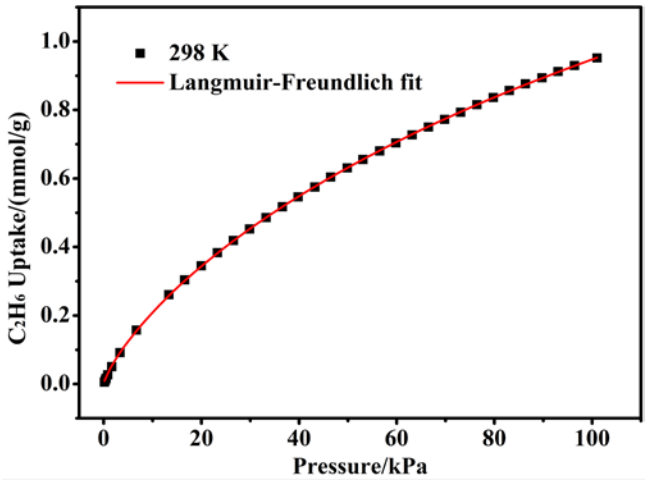

(b)

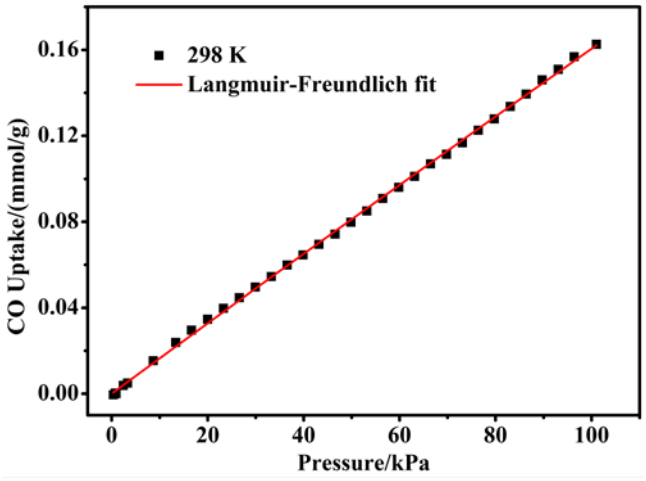

(c)

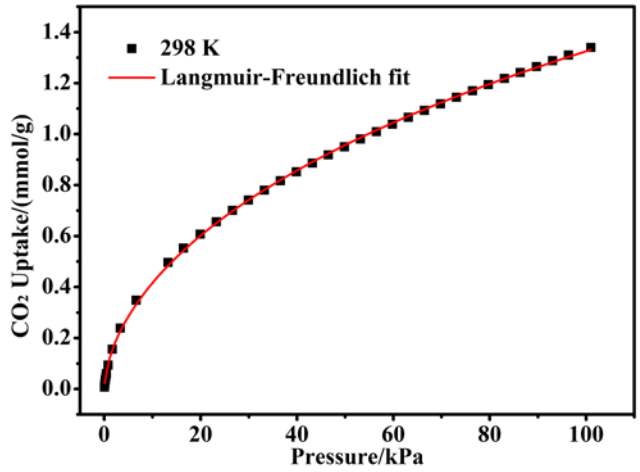

(d)

Figure S5. (a) CH_4 adsorption isotherms of **1** at 298 K with fitting by L-F model: a = 1.74062, b = 0.00195, c =0.94629, Chi^2 = 5.24957×10^{-7}, R^2 = 0.99991; (b) C_2H_6 adsorption isotherms of **1** at 298 K with fitting by L-F model: a = 3.02151, b = 0.01208, c = 0.78875, Chi^2 = 5.21576×10^{-6}, R^2 = 0.99995; (c) CO adsorption isotherms of **1** at 298 K with fitting by L-F model: a = 14.8031, b = 1.13792×10^{-4}, c = 0.99198, Chi^2 = 1.48437×10^{-4}, R^2 = 0.99198; (d) CO_2 adsorption isotherms of **1** at 298 K with fitting by L-F model: a = 5.75588, b = 0.02028, c =0.58426, Chi^2 = 8.01016×10^{-5}, R^2 = 0.99959.

Calculation of sorption heat for CO_2 uptake using Virial 2 model

$$\ln P = \ln N + 1/T \sum_{i=0}^{m} aiN^i + \sum_{i=0}^{n} biN^i \quad Q_{st} = -R\sum_{i=0}^{m} aiN^i$$

The above equation was applied to fit the combined CO_2 isotherm data for **1a** at 273 and 298 K, where P is the pressure, N is the adsorbed amount, T is the temperature, ai and bi are virial coefficients, and m and n are the number of coefficients used to describe the isotherms. Q_{st} is the coverage-dependent enthalpy of adsorption and R is the universal gas constant.

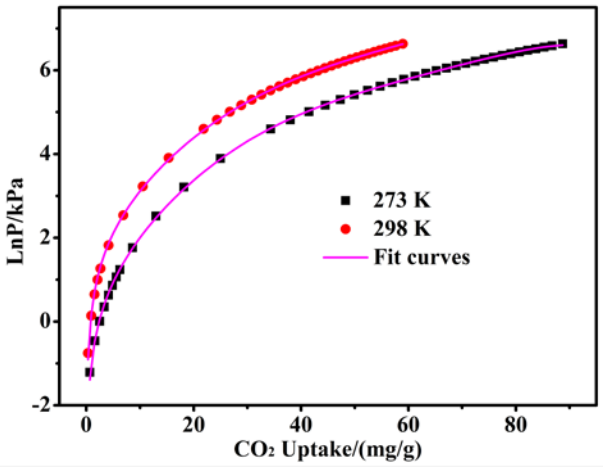

Figure S6. CO_2 adsorption isotherms for **1** fitted by Virial model. Fitging results: a0 = -3994.74156; a1 = 38.87802; a2 = -0.00126; a3 = -0.01342; a4 = 1.83537×10^{-4}; a5 = -8.16535×10^{-7}; b0 = 13.59967; b1 = -0.07245; b2 = 7.73448×10^{-4}; Chi^2 = 0.00146; R^2 = 0.99972.

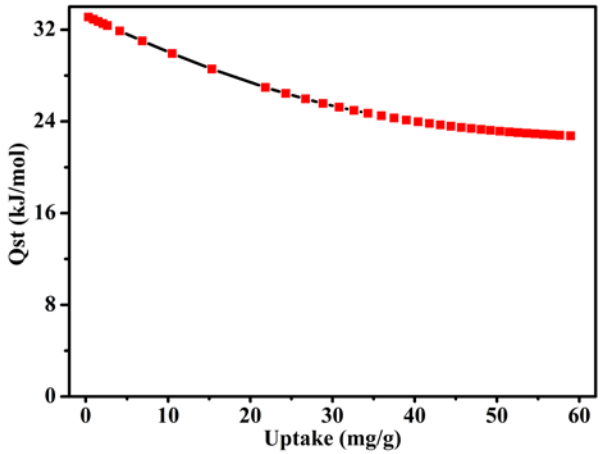

Figure S7. Isosteric heat of CO_2 adsorption for **1** by virial equation.

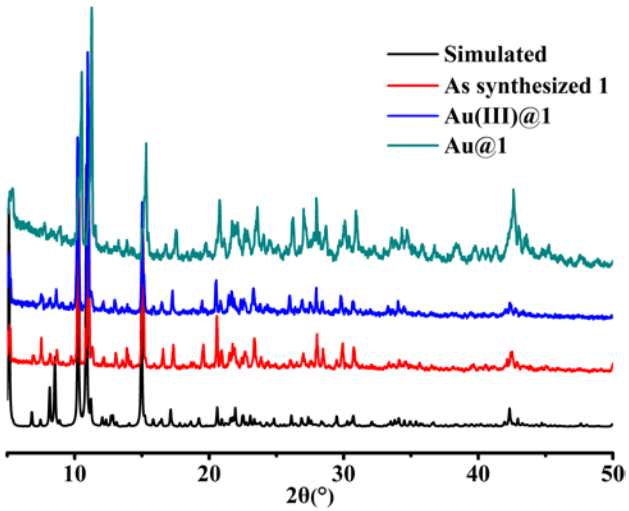

Figure S8. PXRD patterns for the synthesized products, Au(III)@**1** and Au@**1**. The PXRD patterns of different phase match well with the data simulated from the single crystal data,

showing that MOF **1** can keep its original network after series experiments.

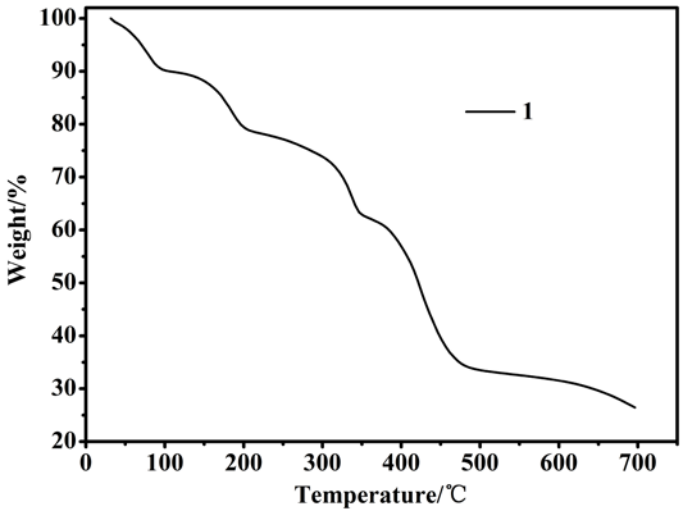

Figure S9. TGA curve for the synthesis products **1**. The TGA curve of **1** begins to have a weight loss before 90 °C, which may be caused by the loss of the guest CH_3CH_2OH solvent molecules. The second weight loss from 90 to 200 °C, corresponding to the removal of the coordination water molecules. And then, the main network start to decomposition when the temperature beyond 200 °C.

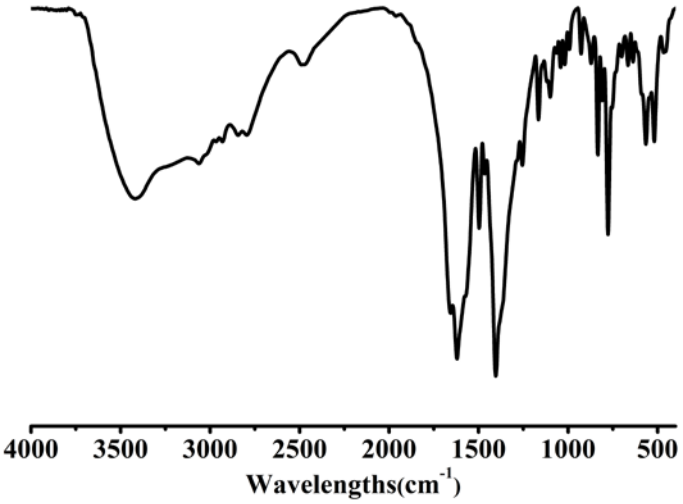

Figure S10. The FT-IR spectrum of **1**.

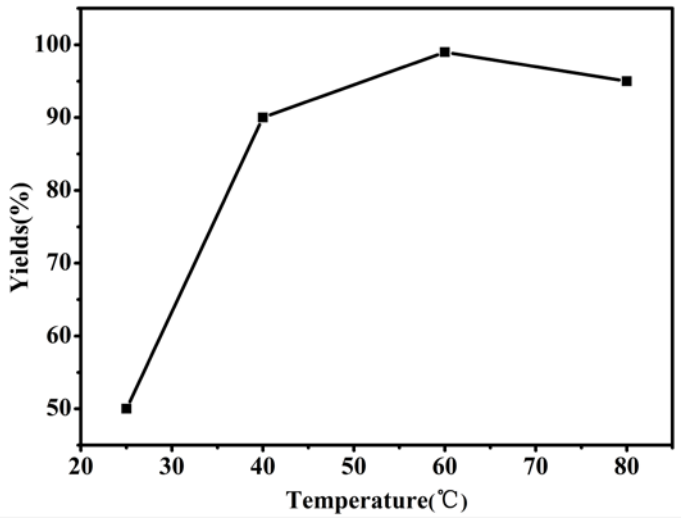

Figure S11. The temperature gradient experiments of the CO_2 cycloaddition.

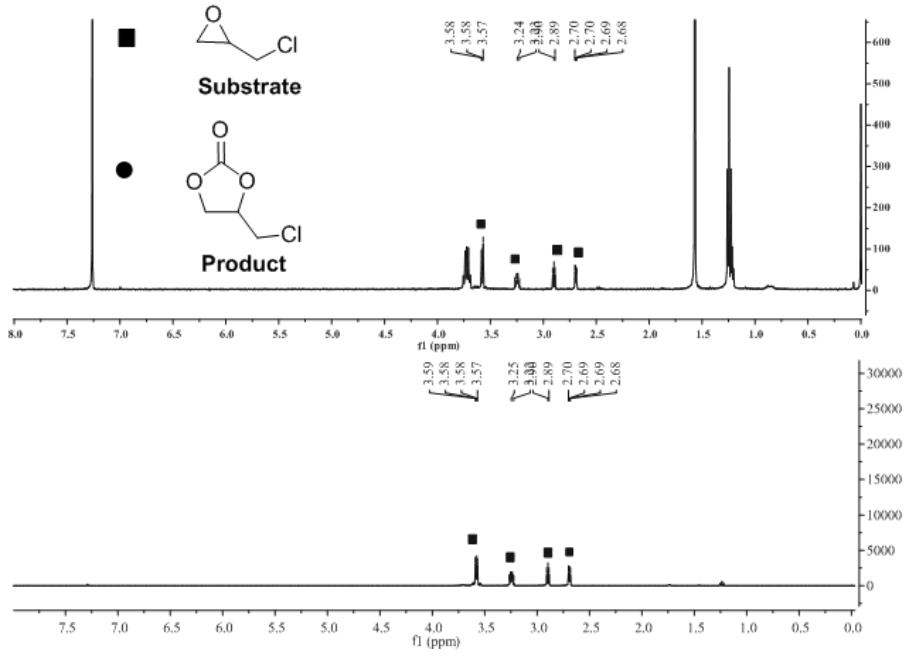

a

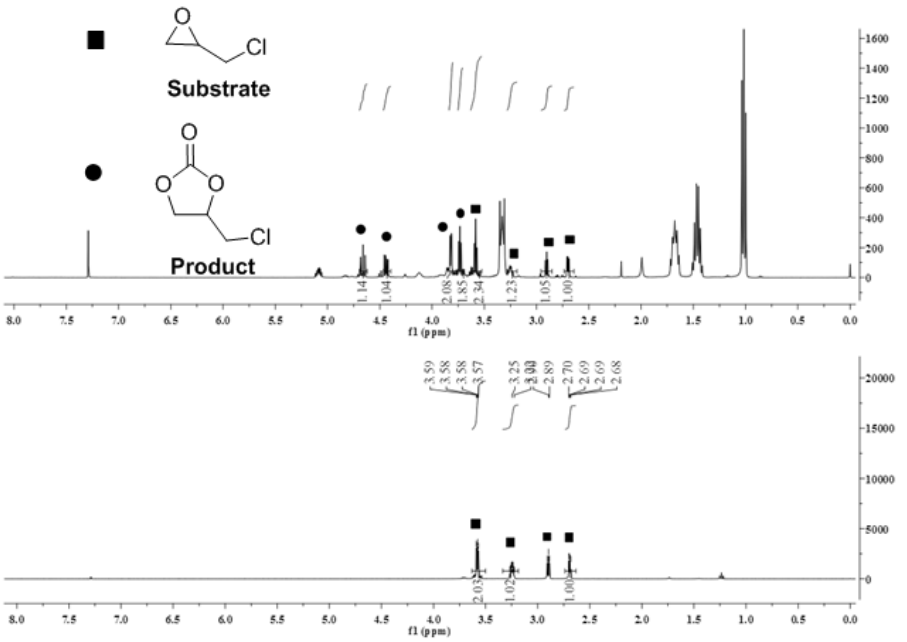

b

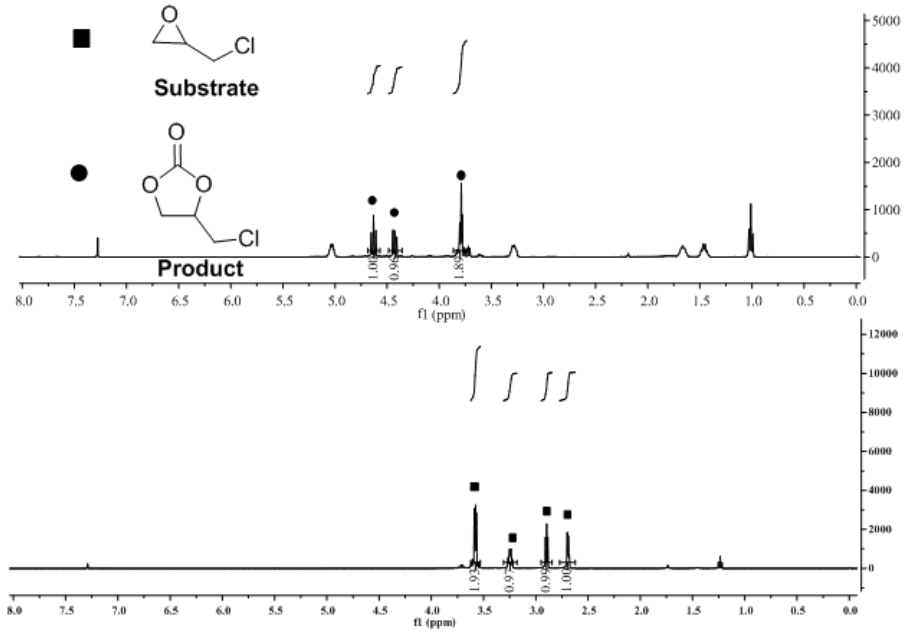

c

Figure S12. H-NMR spectra for the cycloaddition of CO_2 in Table S3 (a-1; b-2; c-3).

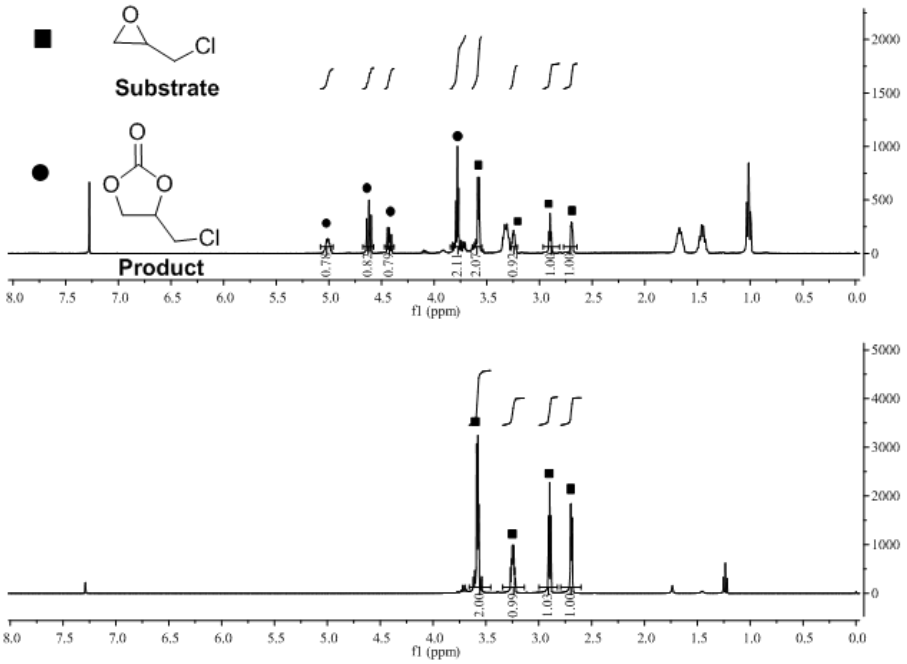

a

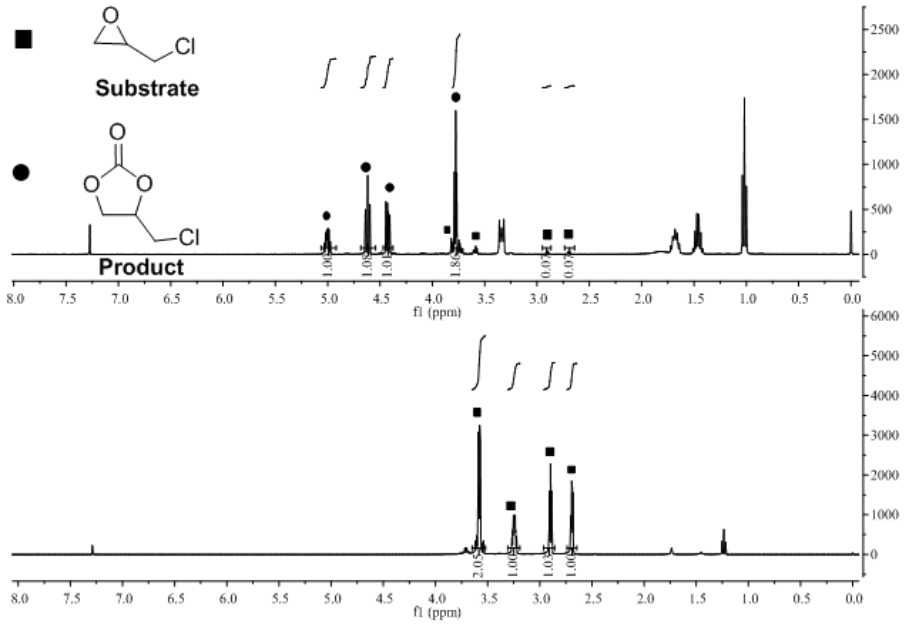

b

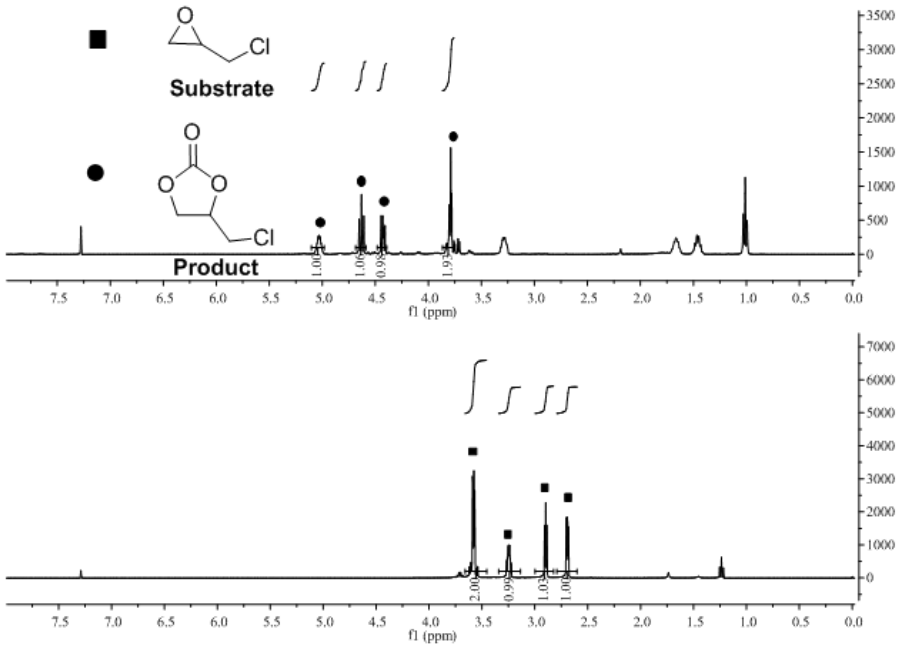

c

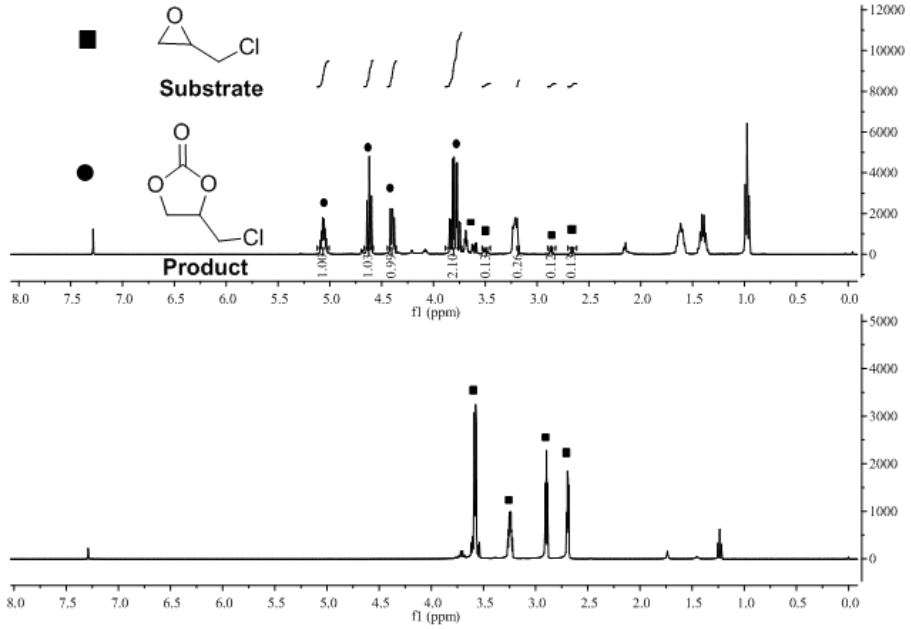

d

Figure S13. H-NMR spectra for the cycloaddition of CO_2 in Table 1 (a-1; b-2; c-3; 4-d).

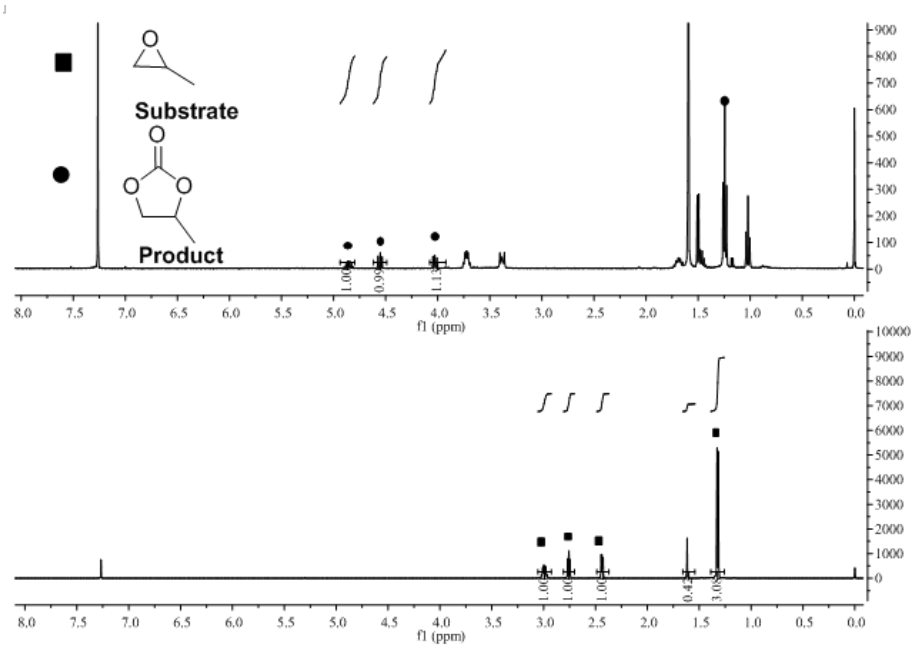

a

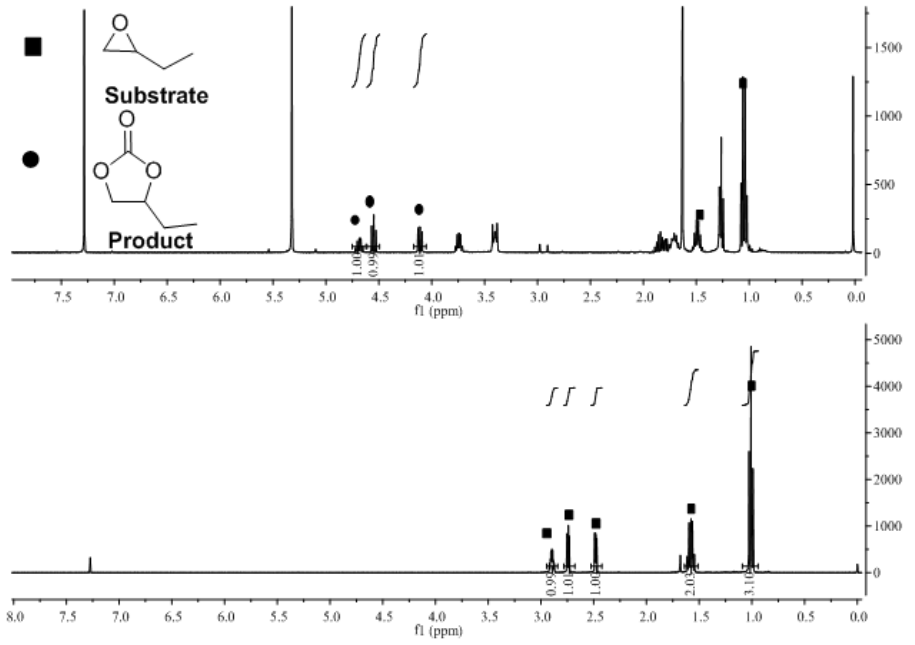

b

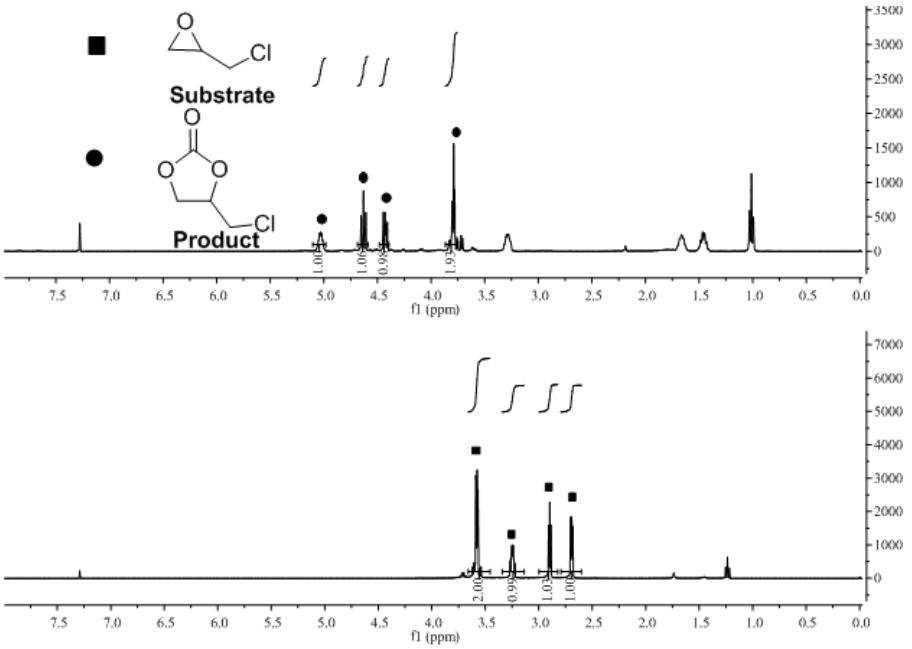

c

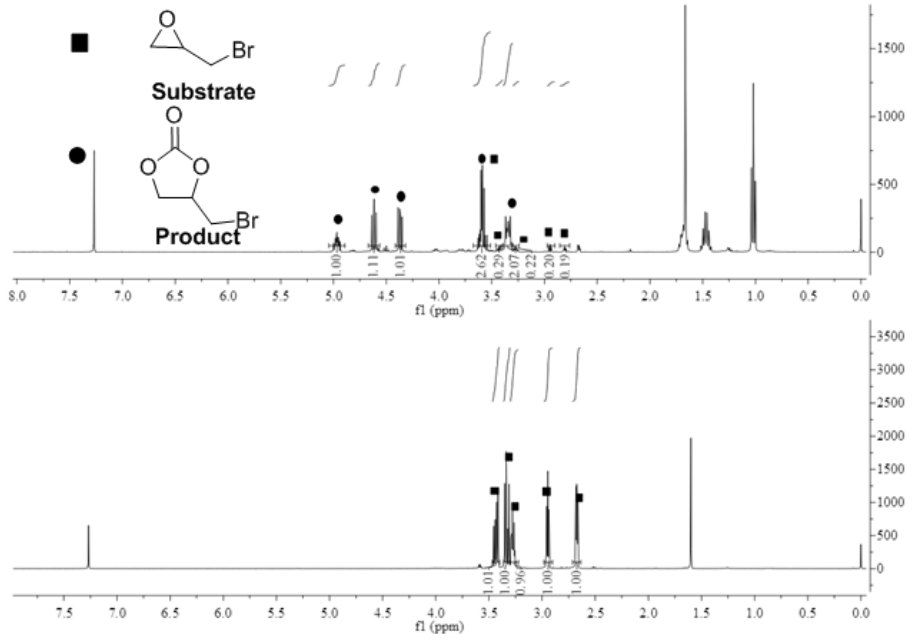

d

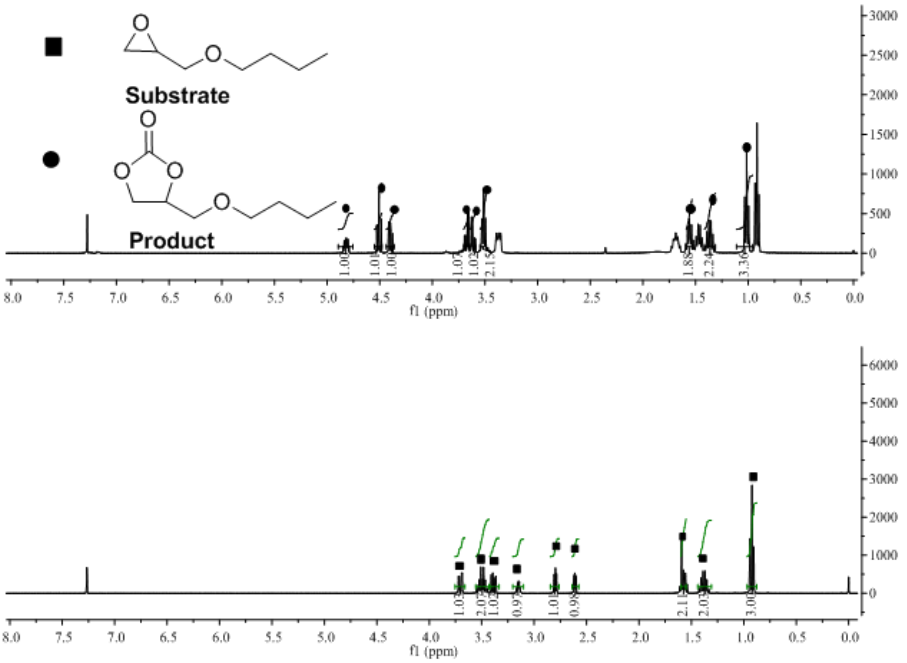

e

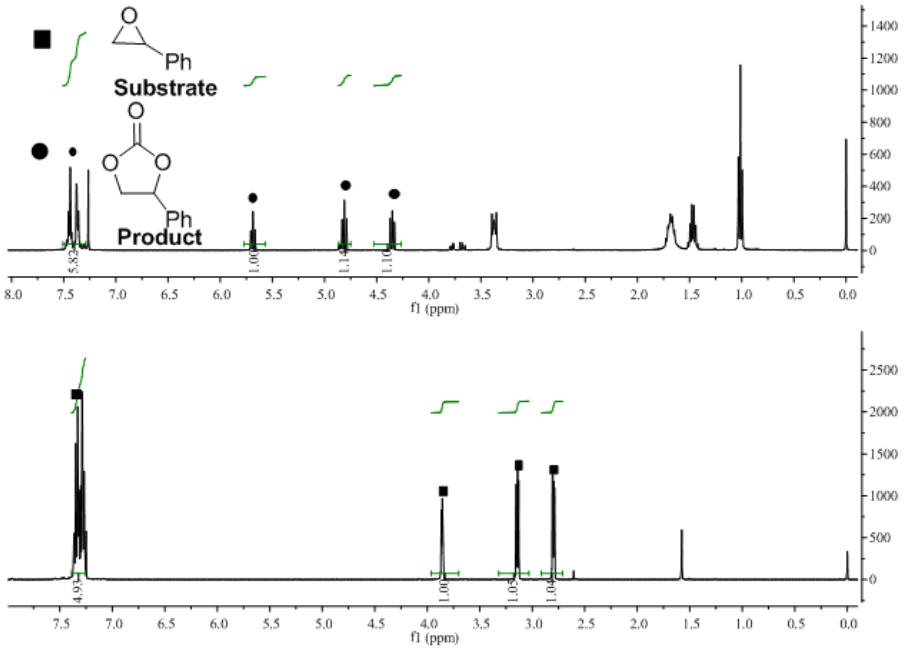

f

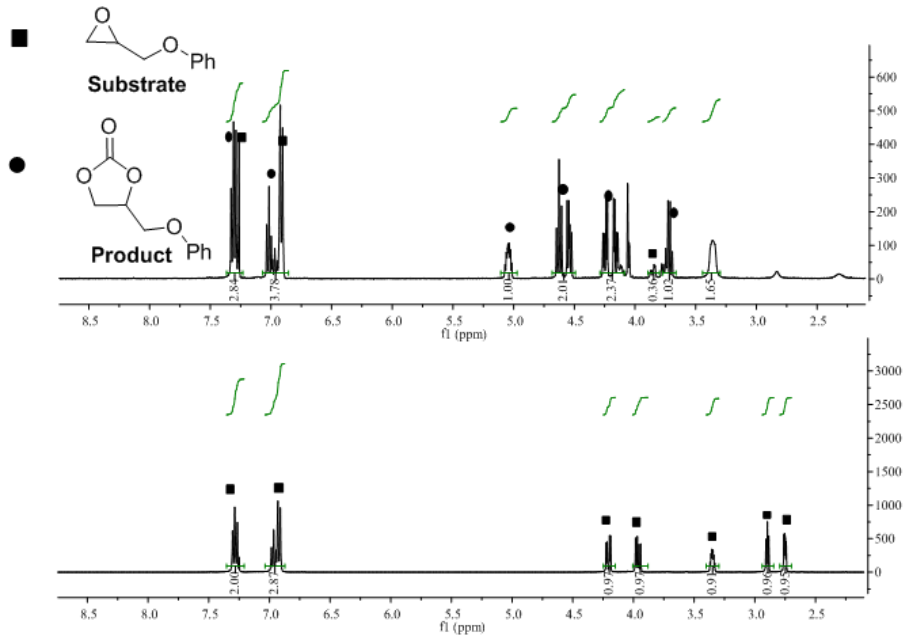

g

Figure S14. H-NMR spectra for the cycloaddition of CO_2 in Table 2 (a-1; b-2; c-3; d-4; e-5; f-6; g-7).

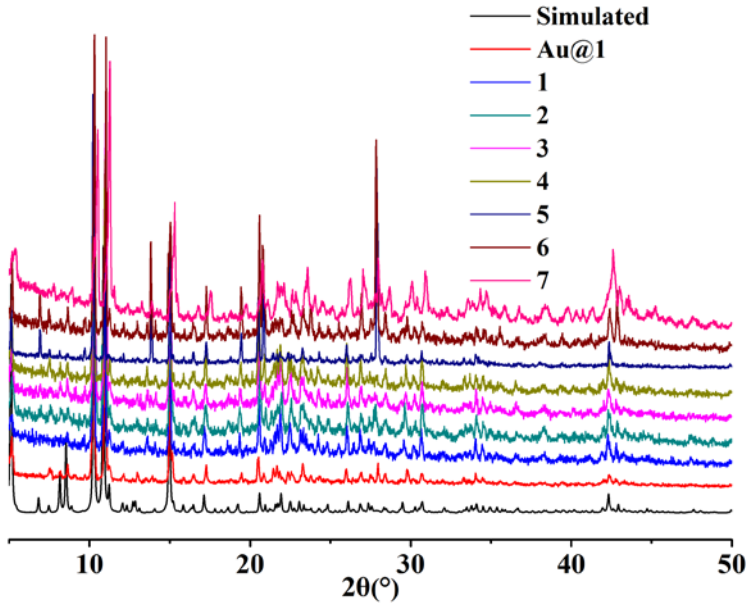

Figure S15. The PXRD patterns of the synthesized products Au@**1** and the composites 1~7 after the cycloaddition of CO_2 with different epoxides [R: -CH_3 (1); -C_2H_5 (2); -CH_3-Cl (3); -CH_3-Br (4), -CH_2-O-C_4H_9 (5), -Ph (6), -CH_2-O-Ph (7)].